Received: 9 January 2023 | Revised: 20 April 2023 | Accepted: 22 April 2023

DOI: 10.1002/nano.202300005

RESEARCH ARTICLE

Nano Select Open Access WILEY

Development of biocide coated polymers and their antimicrobial efficacy

Rowan Watson[1] | **Maria Maxwell**[1] | **Sophie Dunn**[1] | **Alexander Brooks**[2,3] | **Long Jiang**[2] | **Harriet J. Hill**[3] | **Georgia Williams**[1] | **Anna Kotowska**[2] | **Naa Dei Nikoi**[2] | **Zania Stamataki**[3] | **Manuel Banzhaf**[1] | **David Scurr**[2] | **Jack Alfred Bryant**[1] | **Felicity de Cogan**[2]

[1]Institute of Microbiology and Infection, University of Birmingham, Birmingham, UK

[2]School of Pharmacy, University of Nottingham, Nottingham, UK

[3]Institute of Immunology and Immunotherapy, University of Birmingham, Birmingham, UK

Correspondence
Felicity de Cogan, School of Pharmacy, University of Nottingham, Nottingham, UK.
Email: felicity.decogan@nottingham.ac.uk

Abstract

Microbial contamination of plastic surfaces is a significant source of hospital-acquired infections. To produce antimicrobial surfaces, chlorhexidine was attached to nitrided acrylonitrile butadiene styrene (ABS). The uniformity of chlorhexidine distribution on the plastic surfaces was revealed by time-of-flight secondary ion mass spectrometry (TOF-SIMS) imaging. Its antimicrobial efficacy was established against model pathogenic Gram-positive and Gram-negative bacteria, fungi, and viruses. The stability of the bonded chlorhexidine was evaluated via a leaching test. The surfaces rapidly killed microbes: no viable colonies of *Escherichia coli*, *Staphylococcus aureus*, or *Candida albicans* were recoverable after 45 minutes. It was effective against SARS-COV-2, with no viable virions found after 30 minutes. Additionally, the surfaces were as effective in killing chlorhexidine-resistant strains of bacteria as they were in killing naïve strains. The surface was stable; after 2 weeks of leaching, no detectable chlorhexidine was found in the leachate. We believe that the technology is widely applicable to prevent the spread of fomite infection.

KEYWORDS

antibacterial, antimicrobial, $C_7H_4N_2Cl^-$, chlorhexidine, coating, surfaces

1 | INTRODUCTION

Plastics are ubiquitous in the modern world due to their low cost, ease of installation, durability, strength, and versatility.[1] These materials have multiple applications in a healthcare environment in items such as catheters, intravenous bags and devices, dialysis tubing, disposable syringes, gloves, implanted devices, and hospital beds.[2] Several microbial species can survive in a hospital setting despite enhanced cleaning regimes, leading to an increased risk of patients contracting a nosocomial infection.[3] As such, it is critical that microbial survival in the clinic, including the role that plastic surfaces play, is investigated and that methods to eliminate this potential route of infection are explored.

Microorganisms can survive and remain infectious on abiotic surfaces, including plastic surfaces, for extended periods, sometimes up to several months. For example, methicillin-sensitive and methicillin-resistant strains of *Staphylococcus aureus* can survive on polyethylene for more than 90 days,[4] and *Escherichia coli* can survive for up to 11 days on polyethylene and up to 15 days on polyurethane surfaces. In addition, species of the *Acinetobacter* genus have been found to remain viable on plastic surfaces for over 2 months[5]; this is of grave concern, as *Acinetobacter* species are associated with infections in the hospital environment, and multidrug resistance is increasingly prevalent in these species.[6] Pathogenic fungi, such as *Candida albicans*, can survive on polyurethane for up to 6 days, while *Aspergillus fumigatus* can remain on the surface for more than 30 days.[7] The capacity of *Cryptococcus* species to persist and remain infectious on plastic has not yet been assessed; however, their ability to form biofilms on plastic surfaces, including medical devices, has been described, presenting a possible route for infection and persistence.[8,9] SARS-CoV-2, the virus responsible for causing COVID-19, has been found to remain infectious on plastic surfaces for up to 7 days.[10,11] As such, the surfaces present in an environment can transmit pathogenic microorganisms, which is of the utmost concern in healthcare settings.

The COVID-19 pandemic has drawn increased attention to hospital-acquired infections, as it has been estimated that 20% of all patients hospitalized with COVID-19 contracted the virus while already in hospital.[12] It has been estimated that in 2016/2017, 4.7% of adult hospital inpatients contracted a nosocomial infection, with 22,800 patients dying due to these infections despite these deaths being preventable. The most common pathogens that cause hospital-acquired infections are *E. coli*, *S. aureus*, and *Clostridium difficile*, with nosocomial infections typically manifesting as urinary tract, surgical site, gastrointestinal, or bloodstream infections.[13] Outbreaks of nosocomial infections in the clinic are frequently caused by strains resistant to antimicrobial drugs, for example, methicillin-resistant *S. aureus* (MRSA) and vancomycin-resistant *Enterococcus* (VRE). MRSA infection rates rose throughout the 1990s and into the early 2000s in the United Kingdom. MRSA is now considered endemic in British hospitals, with 1652 patients dying from MRSA infection in 2006.[14,15] Reductions in the incidence of MRSA infection have been attributed to mandatory reporting practices, public information campaigns, and enhanced cleaning regimes.[16] Despite these improvements, research has shown that contaminated surfaces, including plastic surfaces, can act as a reservoir of antimicrobial resistance genes, encouraging the spread of antimicrobial resistance across bacterial species through horizontal gene transfer despite deep cleaning practices.[17] It is paramount that new technologies are developed to prevent the spread of pathogenic microorganisms to vulnerable patients and address the ever-increasing threat of antimicrobial resistance.

Antimicrobial surfaces have been developed to prevent the contamination of abiotic surfaces by pathogenic species, and some of these have been used in a clinical setting with success. Some of these surfaces operate on the principle of preventing microbial attachment to the surface, such as using polyethylene glycol as an antifouling agent. When applied to a surface, polyethylene glycol confers hydrophilicity to the material, repelling bacteria, and preventing attachment and biofilm formation.[18,19] Diamond-like carbon films are an alternative to polyethylene glycol coating; these have been used to develop antimicrobial surfaces, preventing bacterial adhesion and biofilm formation through hydrophilic action.[20] Due to their biocompatibility, durability, and resistance to friction, their potential use for medical implants has been extensively investigated.[21,22] Diamond-like carbon films are especially attractive due to their ability to be ''doped'' with antimicrobial compounds, for example, silver or copper, conferring even greater antimicrobial efficacy.[23]

Other antimicrobial surfaces are designed to release biocides to kill pathogenic microorganisms. For example, triclosan, an antibacterial and antifungal agent, has been used to coat surfaces in a clinical setting and is highly effective at killing pathogens, although triclosan has no antifouling activity.[24] Despite this, there are concerns about triclosan resistance, which has previously been described in pathogenic bacteria,[25] especially as triclosan resistance appears to be correlated with cross-resistance to other antibiotics.[26] These findings raise questions about the long-term usage of triclosan coatings.

We have previously shown the possibility of grafting peptides onto steel surfaces to confer antimicrobial properties to these materials.[27] We have also shown that steel and air filters can be coated with the broad-spectrum biocidal agent chlorhexidine digluconate (CHDG) to develop antimicrobial surfaces that are efficacious against a range of pathogenic bacteria, fungi, and viruses.[28,29] Unlike previously developed biocide-coated technologies, this does not rely on biocide release for functional activity. In this study, we demonstrate the ability to extend this coating technology to plastic, creating surfaces that are highly effective against Gram-positive (*S. aureus*) and Gram-negative bacteria (*E. coli*), pathogenic fungi, and viruses, including SARS-CoV-2 as well as displaying durability against leaching.

2 | MATERIALS AND METHODS

Absolute ethanol was purchased from Fisher Scientific. *N*,*N*-Diisopropylethylamine (DIEA) was obtained from Alfa Aesar, and 2-(1H-benzotriazol-1-yl)−1,1,2,3-tetramethyluronium hexafluorophosphate (HBTU) from Cambridge Reagents. Phosphate-buffered saline (PBS) was purchased from Gibco as tablets: a working solution was prepared using deionized water per the manufacturer's instructions. Zirconium oxide beads (0.15 mm diameter) were obtained from Thistle Scientific UK: 7–10 beads would be placed in an autoclavable 15 mL centrifuge tube (Eppendorf) and autoclaved to produce sterile beads. Chlorhexidine (20% chlorhexidine digluconate in water), Muller Hinton Broth (MHB), Luria-Bertani Broth (LB), Dey-Engley Neutralizing Broth, yeast extract, peptone, agar powder, and anhydrous glucose were all purchased from Sigma Aldrich UK. Nitride-treated acrylonitrile butadiene styrene (ABS) plastic and control ABS were provided by NitroPep Ltd.

2.1 | Coating of polymer surfaces with chlorhexidine

A saturated solution of HBTU was prepared by dispersing 2 g of HBTU in 10 mL ethanol. The plastic samples were cut into pieces approximately 1 cm x 1 cm; they weighed approximately 0.5 g. Individual nitrided or control plastic pieces were placed in 15 mL polypropylene centrifuge tubes and washed in 3 mL of ethanol. The ethanol was discarded, and a fresh 3 mL aliquot was added. Then 600 μL of DIEA, 1 mL of HBTU solution, and 200 μL of chlorhexidine were added to the tube. The tube was capped, and the samples were gently oscillated on a rotary shaker at room temperature for 1 hour. The surfaces were then washed using literature protocols to ensure no unbound material remained on the surface.[30] Briefly, the samples were washed 5 times in 3 mL of deionized water and 3 times in 3 mL of PBS. Finally, the surfaces were air-dried and stored in the dark at room temperature (18–22°C) for analysis.

2.2 | ToF SIMS

ToF-SIMS spectra were acquired using a ToF V (IONTOF GmbH) instrument. A 30 keV Bi^{3+} primary beam was used to acquire liquid metal ion gun (LMIG) ToF-SIMS images. The LMIG current was 0.05 pA, and the ToF image was run on an area of 400 × 400 μm using random raster mode with a 256 × 256-pixel density. The cycle time was set to 180 μs. The optimal target potential was set to −57.5 V. Three separate areas were analyzed on each sample, and each measurement lasted 15 scans; the total ion dose per measurement was 9.44×10^{10}.

2.3 | Water contact angle measurements

The samples were prepared as previously described, and the water contact angle (WCA) was measured by a CAM 200 Optical Contact Angel Meter (KSC Instruments Ltd.) using a sessile drop method. Microliter droplets of deionized water (resistivity = 18.2 MΩ cm^{-1}) were used for the measurements. Measurements were performed in 20 locations (five for each plastic piece). The WCA values were obtained using Young-Laplace fitting.

2.4 | Antimicrobial efficacy testing

2.4.1 | Antibacterial efficacy testing

Both *E. coli* K-12 BW25113 and *S. aureus* ATCC6538 were cultured in 5 mL LB broth overnight at 37°C for ≈18 h with shaking (180 rpm) before being adjusted to ≈1×10^9 (colony-forming units) CFU mL^{-1}. For each condition assessed, three samples were placed in individual wells of a 12-well plate and inoculated with the bacterial suspensions arrayed in a 3 × 3 grid of 1 μL aliquots onto the sample surfaces. The well plate lid was replaced, and the samples were then incubated at room temperature for either 1, 15, 30, or 45 minutes. Following incubation, the samples were removed from the 12-well plate and placed in 15 mL centrifuge tubes containing sterile zirconium beads. To recover bacteria from the surfaces, 10 mL sterile Dey-Engley Neutralizing Broth was added to the surfaces and zirconium beads, and the mixture was vortex mixed for 1 minute. The neutralizing broth suspension was then serially diluted 1:3 eight times in sterile PBS utilizing a 96-well plate, and three 10 μL spots from each dilution were plated on LB agar plates. Survival was assessed by counting CFU after incubation for 16–18 h at 37°C. All dilutions were accounted for and corrected when calculating CFU by multiplying the colony number by the relevant dilution factor. The limit of detection for the assay is 1×10^3 CFU.

2.4.2 | Antifungal efficacy testing

C. albicans SC5314 samples were cultured in 5 mL YPD broth (1% yeast extract, 2% bacto-peptone, and 2% glucose) overnight at 30°C for ≈18 hours with shaking (180 rpm) before being adjusted to ≈1×10^8 CFU mL^{-1}. For each condition assessed, three samples were placed in individual wells of a 12-well plate and inoculated with the fungal

suspensions. Fungal cultures were pipetted onto test surfaces as 9×1 μL drops in a simulated splash test ($\approx 1 \times 10^6$ cells per surface). The lid of the well plate was replaced, and surfaces were incubated at room temperature for either 1, 15, 30, or 45 minutes. Following incubation, the samples were removed from the 12-well plate and placed in 15 mL centrifuge tubes containing sterile zirconium beads. To recover fungi from the surfaces, 10 mL sterile Dey-Engley Neutralizing Broth was added to the surfaces and zirconium beads, and the mixture was vortex mixed for 1 minute in neutralizing broth suspension was serially diluted 1:3 eight times in sterile PBS utilizing a 96-well plate. Three 10 μL spots from each dilution were plated on YPD agar plates. Survival was assessed by counting CFU after incubation at 30°C for 18–24 hours. All dilutions were accounted for and were corrected when calculating CFU by multiplying the colony number by the relevant dilution factor. The limit of detection for the assay is 1×10^3 CFU.

2.4.3 | Antiviral efficacy testing

Coated and control surfaces were placed in separate 15 mL centrifuge tubes, and 10 μL of viral stock (SARS-CoV-2-England 2 (Wuhan strain) virus at 10^6 IU mL^{-1} (GSAID Accession ID EPI_ISL_407073)) was added to each. The samples were incubated for 5 min at room temperature. Two hundred μL of viral culture media (Dulbecco's Modified Eagle's Medium, DMEM, Gibco) was added to each cryovial, and the vial was agitated gently to wash the surfaces. Fifty microliters of the supernatant was incubated in separate wells in a black 96-well flat-bottomed polystyrene imaging plate (Greiner) seeded with 4×10^4 Vero cells per well. The Vero cells were cultured in DMEM supplemented with 10% fetal bovine serum, 2 mM L-glutamine, 100 U mL^{-1} penicillin, 10 μg mL^{-1} streptomycin, and 1% non-essential amino acids (culture media) for 48 hours at 37°C. The cells were maintained at 37°C and 5% CO_2. Finally, the media was removed and discarded, and the cells were fixed in ice-cold methanol for 5 min. The Vero cells were then washed in PBS, stained with rabbit anti-SARS-CoV-2 spike protein, subunit 1 (CR3022, The Native Antigen Company), and detected by Alexa Fluor 555-conjugated goat anti-rabbit IgG secondary antibody (Invitrogen, Thermo Fisher Scientific). The cell nuclei were counter-stained with Hoechst 33342 (Thermo Fisher Scientific). The cells were given a final wash in PBS and then imaged and analyzed using a Thermo Scientific CellInsight CX5 high-content screening (HCS) platform. Infected cells and cell viability were detected by measuring perinuclear fluorescence above a threshold determined by positive (untreated) and negative (uninfected) controls.

2.5 | Generation of chlorhexidine-resistant bacteria

The minimum inhibitory concentration (MIC) for chlorhexidine digluconate (CHDG) against *E. coli* K12 BW25513 and *S. aureus* ATCC6538 was established by a broth microdilution assay in Mueller-Hinton Broth (MHB).[31] Briefly, the strains were cultured overnight for ≈16–18 hours in MHB at 37 °C and shaking set to 180 rpm. The culture was diluted to 1×10^9 CFU mL^{-1}, and the above microdilution protocol was performed using six wells of a 96-well plate, with a total of five repeats for each strain. CHDG was diluted to a desired concentration in MHB and serially diluted one in two in MHB. Each well was inoculated with the diluted bacterial culture, and the well plate was sealed with a breathable membrane and incubated in a static incubator overnight at 37 °C. The next day, the plate was removed from the incubator, and the MIC was determined through reading absorbance at 600 nm; the MIC is the lowest concentration of CHDG at which bacterial growth is completely suppressed. The membrane was cut away from the first well showing bacterial growth, and a 1:1000 dilution of this culture in MHB was obtained; a glycerol stock solution of this culture was also created, so a fossil record of the experiment could be maintained.

To continue with the evolution of resistance, CHDG was diluted in MHB to a concentration four times greater than the MIC obtained earlier and was serially diluted one in two in MHB in a 96-well plate, as described above. Each test well was inoculated with the diluted culture obtained following the reading of bacterial absorbance, and the plate was sealed with a breathable membrane and incubated in a static incubator overnight for ≈16–18 hours at 37 °C. This protocol was continued until a significantly elevated MIC value was obtained. At this point, the MIC values could be confirmed for each generated strain through the resurrection of the glycerol-preserved strains. The antimicrobial efficacy of the chlorhexidine-coated polymer surfaces against chlorhexidine-resistant *E. coli* and *S. aureus* was determined as described in the "Antibacterial Efficacy Testing" section.

2.6 | Leaching of chlorhexidine from the surface coating

Prior to testing, the surfaces were washed following literature protocols by Naderi et al. to ensure the unbound coating solution was removed.[30] This was followed by immersion of the surfaces in 10 mL of PBS. Samples were stored at room temperature in the dark. At 24-hour

intervals, 200 μL of each PBS solution was removed, and the absorbance was measured at 280 nm. To assess if the leachate had antimicrobial efficacy, the leachate was diluted 1:10, and 9 μL of a culture of *E. coli* BW25113 diluted to OD = 1.0 (equivalent to 10^{-9} CFU) was added to each solution and was incubated at room temperature for 14 days. Prior to testing, the surfaces were washed to ensure unbound coating solution was removed as described above; this was followed by immersion of the surfaces in 10 mL of PBS. Samples were stored at room temperature in the dark. At 24-hour intervals, 200 μL of each PBS solution was removed, and the absorbance was measured at 280 nm on a Clariostar FLUOstar Omega, BMG Labtech microplate reader. The assay was sensitive to chlorhexidine to a concentration of 2.2 μM. To assess if the leachate had antimicrobial efficacy, the leachate was serially diluted 1:10 in sterile PBS utilizing 1.5 mL microfuge tubes to a 10^{-9} concentration, and 9 μL of a culture of *E. coli* BW25113 diluted to OD = 1.0 was added to each solution. Each inoculated solution was incubated at room temperature for 1 hour. The inoculated leachate solutions were serially diluted 1:3 in sterile PBS, and bacterial survival was calculated following counting CFU following incubation for 16–18 hours at 37 ˚C on LB agar. All dilutions were accounted for and were corrected when calculating CFU by multiplying the colony number by the relevant dilution factor. The bacteria were sensitive to a concentration of 1 μM or greater chlorhexidine.

To assess if the plastic surfaces retained antimicrobial efficacy post-leaching, the surfaces were inoculated with 9 × 1 μL of a culture of *E. coli* BW25113 diluted to OD = 1.0 in a simulated splash test. Following incubation for 30 minutes, the bacteria were recovered from the surfaces by transferring each surface to a tube containing 10 mL of Dey-Engley Neutralizing Broth and 7–10 sterile zirconium beads and vortex mixed for 1 minute. The bacterial suspension was then serially diluted 1:3 in sterile PBS, and bacterial survival was calculated by counting CFU following a 16–18 hours incubation at 37 ˚C on LB agar.

Finally, the surfaces were imaged pre- and post-leaching using white light microscopy to examine the effects of the leaching protocol on the surface integrity. The surfaces were imaged using a Zeiss Axio Zoom V16 microscope equipped with a Zeiss Axiocam 503 Mono camera. The surfaces were imaged at 6.3×, 32×, and 56× magnification.

2.7 | Data analysis

All tests were performed three times in triplicate. Statistical analysis was performed using SPSS (Version 28.0.1.1[14]; IBM). Data were analyzed using an independent samples *t*-test, and α was set to 0.05.

3 | RESULTS

3.1 | Surface coating characterization

The presence and uniformity of the chlorhexidine coating across the polymer surfaces were monitored using ToF-SIMS. Chlorhexidine was identified using the established $C_7H_4N_2Cl^-$ peak for molecular identification.[32,33] The normalized ion intensity quantification averages for the treated samples had a mean ion intensity of 0.031 ± 0.002, significantly higher ($p < 0.01$) than the control samples, which had a mean of 0.002 ± 0.0002 (Figure 1A). Scans across the surfaces showed uniform distribution of the $C_7H_4N_2Cl^-$ ion across the treated samples (Figure 1B) and little ion presence across the control surfaces (Figure 1C).

The surface water contact angle was measured to determine the effect of the coating on surface hydrophobicity (Figure 2). Uncoated surfaces were hydrophobic with a mean water contact angle of 83.5 ± 4.7°. After coating, the water contact angle was significantly reduced to 46.8 ± 8.3°, $p < 0.001$ (Figure 2).

3.2 | Antimicrobial efficacy

With the presence of chlorhexidine on the surface established, the ability of chlorhexidine to maintain biocidal activity after surface binding was tested. To simulate the real-world contamination of materials, a simulated splash test was used to model low-volume, high bacterial load contamination. Following 1- and 15-minute incubation periods, there were no significant differences in the *E. coli* CFU between the control and treated surfaces (Figure 3A). However, following incubation for 30 minutes, the control surfaces had 6.82 ± 0.04 Log_{10} CFU compared to treated surfaces with only 1.13 ± 0.51 Log_{10} CFU. This demonstrates that the surfaces can achieve a 3-log reduction at 30 minutes. At 45 minutes, the differences are even more pronounced as control surfaces still had 7.27 ± 0.02 Log_{10} CFU, whereas treated surfaces had no countable surviving bacteria on the surfaces. These results were statistically significant, with $p < 0.001$ after 30 minutes.

The antimicrobial effect against the model Gram-positive organism *S. aureus* ATCC6538 was more pronounced, with a 1-log reduction observed after 60 seconds (Figure 3B). Control surfaces had 6.3 ± 0.15 Log_{10} CFU detectable on the surfaces, whereas the treated surfaces had dropped to 4.27 ± 0.51 Log_{10} CFU. Survival on the control surfaces was consistent across the time course. In

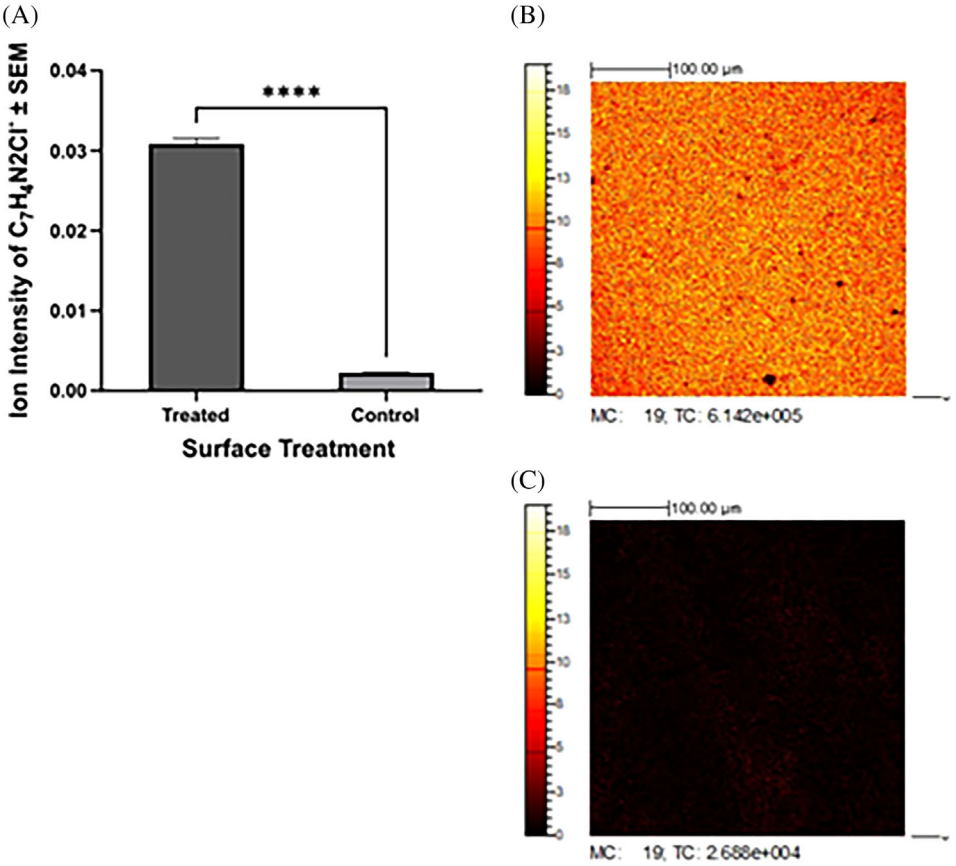

FIGURE 1 Surface characterization of treated polymer surfaces. A) Quantification of ion intensity across the surfaces comparing treated and control surfaces, $n = 3$, error bars show standard deviation, ** denotes statistical significance <0.01. B) Scan across the treated surface showing ion intensity relating to the $C_7H_4N_2Cl^-$ peak. Image is representative of all images taken on all samples. C) Scan across the control surface showing ion intensity relating to the $C_7H_4N_2Cl^-$ peak. Image is representative of all images taken on all samples.

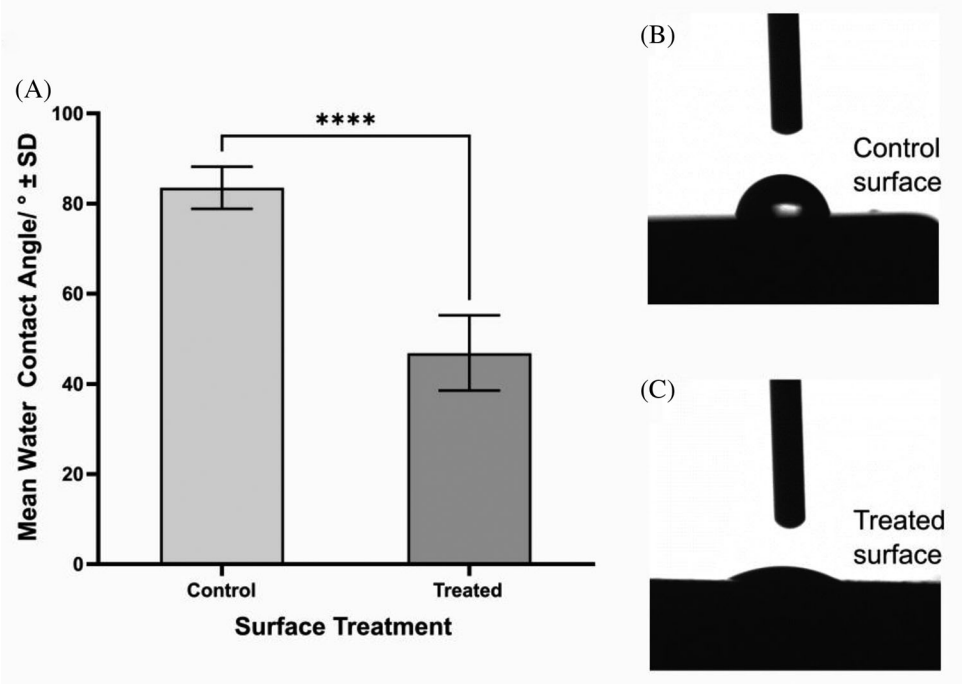

FIGURE 2 Water contact angle measurements of treated and control surfaces. Quantification showing the comparison of the mean of all readings taken, $n = 4$, error bars show standard deviation and *** denotes that $p < 0.001$.

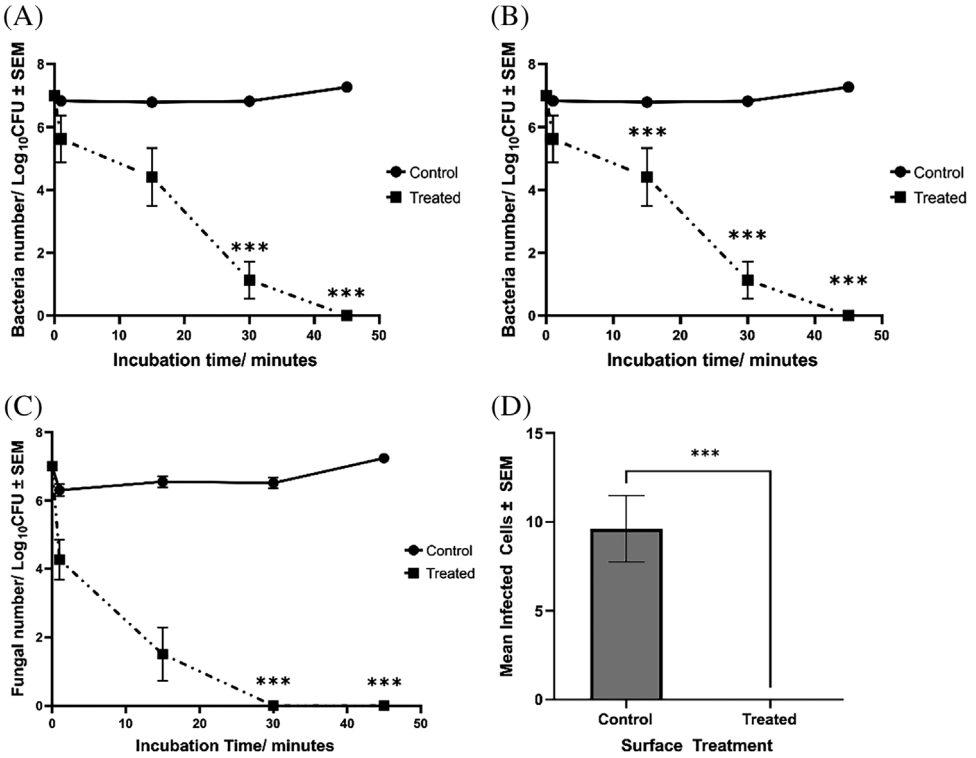

FIGURE 3 Antimicrobial efficacy of control and treated surfaces. **A**) Time course showing *E. coli* survival at different time points following incubation on untreated and CHDG treated surfaces. *** denotes statistical significance < 0.001, $n = 9$. Error bars show standard error of the mean. **B**) Time course showing MRSA survival at different time points following incubation on untreated and treated surfaces. *** denotes statistical significance < 0.001, $n = 9$. Error bars show standard error of the mean. **C**) Time course showing *C. albicans* survival at different time points following incubation on untreated and treated surfaces. *** denotes statistical significance < 0.001, $n = 9$. Error bars show standard error of the mean. D) Time course showing antiviral efficacy of the surfaces at SARS-CoV-2 inactivation at different time points following incubation on untreated and CHDG treated surfaces. *** denotes statistical significance < 0.001, $n = 9$. Error bars show standard error of mean.

contrast, the mean number of recoverable cells on treated surfaces decreased to 1.51 ± 0.67 Log_{10} CFU at 15 minutes, and there were no detectable surviving bacteria at 30 and 45 minutes. These results were also statistically significant, with $p < 0.001$ after 15 minutes.

This demonstrates that the surfaces showed antimicrobial efficacy against both Gram-negative and Gram-positive bacteria, with the effect being more pronounced for the Gram-positive organism.

Surfaces can also be contaminated with opportunistic fungal pathogens; therefore, the antifungal efficacy of surface-immobilized chlorhexidine was tested against *C. albicans* SC5314 (Figure 3C). Cells were added to the surface at $\approx 1 \times 10^9$ CFU mL^{-1} and recovered at intervals throughout the time course. There was no significant difference between the treated surfaces (4.42 ± 0.49 Log_{10} CFU) and the control surfaces (5.49 ± 0.03 Log_{10} CFU) after a 1-minute incubation. However, there were no recoverable cells on the treated surfaces at other times. In comparison, the control surfaces showed the stable survival of *C. albicans* throughout the time course.

Having established that the treated polymer surfaces are efficacious in rapidly killing bacterial and fungal species, we then assessed the activity of the technology against the causative agent of COVID-19: SARS-CoV-2 virus (Wuhan strain) (Figure 3D). The simulated splash assay was modified by applying 5×10^4 infectious units (IU) to the test surfaces and incubating for 5 minutes before virions were removed from the surface. The remaining virus particles from the treated or control surfaces were harvested using a cell culture medium, which was then incubated with Vero cells to determine infectivity. The antimicrobial-coated plastic demonstrated excellent antiviral properties, with the rate of infected cells dropping from $9.6\% \pm 3.2\%$ cells observed on the control surfaces to no detectable infected cells on the antimicrobial-coated plastic surfaces.

Antimicrobial resistance is a significant issue when employing antimicrobial technologies; therefore, it is vital to determine the response of novel antimicrobial technologies to resistant bacteria. To ascertain the efficacy of the AMS against resistant bacteria, we first evolved resistance of our naïve strains of *E. coli* and *S. aureus* to chlorhexidine

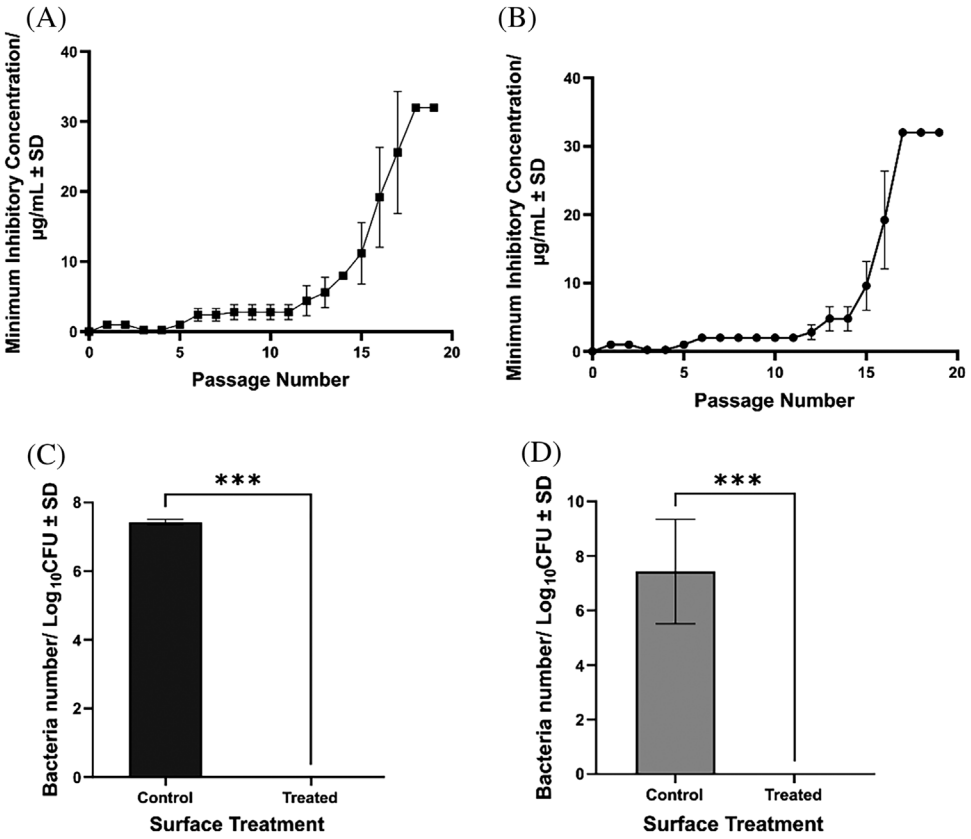

FIGURE 4 Generation of antimicrobial resistant bacteria and surface efficacy against them. A) Effect of passaging *E. coli* in sub-lethal concentration of chlorhexidine on the minimum inhibitory concentration of chlorhexidine for the bacteria, $n = 5$, error bars show standard deviation. B) Effect of passaging *S. aureus* in sub-lethal concentration of chlorhexidine on the minimum inhibitory concentration of chlorhexidine for the bacteria, $n = 5$, error bars show standard deviation. C) Antimicrobial efficacy of control and treated surfaces against chlorhexidine resistant *E coli*. *** denotes statistical significance < 0.001, $n = 9$. Error bars show standard error of the mean. D) Resistant *S. aureus* survival following incubation on untreated and treated surfaces. *** denotes statistical significance < 0.001, $n = 9$. Error bars show standard error of the mean.

in liquid growth media. The original MIC of each strain was 1 µM. Next, bacteria were serially passaged 20 times in the presence of 0.5× MIC chlorhexidine in MHB with aeration. The *E. coli* cultures had a steady increase in MIC until passage 14, after which a significant increase was observed over the following four passages, with the MIC plateauing at 32 µM, which was × times higher than that of the naïve parent strains (give MIC of the original strains) (Figure 4A). A similar pattern was observed with *S. aureus*, where little increase in the MIC was observed until passage 15, after which a significant increase was then seen over the following three passages, with the MIC plateauing again at 32 µM (Figure 4B). The surfaces were then tested against these strains to determine the efficacy of the surface against resistant bacteria. Control surfaces did not affect the resistant *E. coli* strain, whereas no recoverable CFU was observed following incubation of the resistant strain on treated surfaces (Figure 4D). A similar effect was observed for the resistant *S. aureus* strain, with the control surfaces not affecting survival, whereas no cells were recovered following incubation on treated surfaces. This demonstrates that the surfaces are effective against both naïve and chlorhexidine-resistant bacteria (Figure 4D).

3.3 | Surface leaching

Once the antimicrobial efficacy of the surfaces was established, the durability of the surfaces was examined to determine their suitability for use. The surfaces were immersed in PBS for 14 days, and at each timepoint, the absorbance of the leachate from the surface was monitored to determine the presence of chlorhexidine (Figure 5). Chlorhexidine concentrations can be quantified by the suppression of the background fluorescence of polystyrene plates.[34] At day 0, a background reading of 33741 ± 762 a.u. was observed for the solution before adding the control samples and 32084 ± 706 a.u. for the treated samples. There was no significant increase for the treated samples up to and including day 14, with the measurements remain-

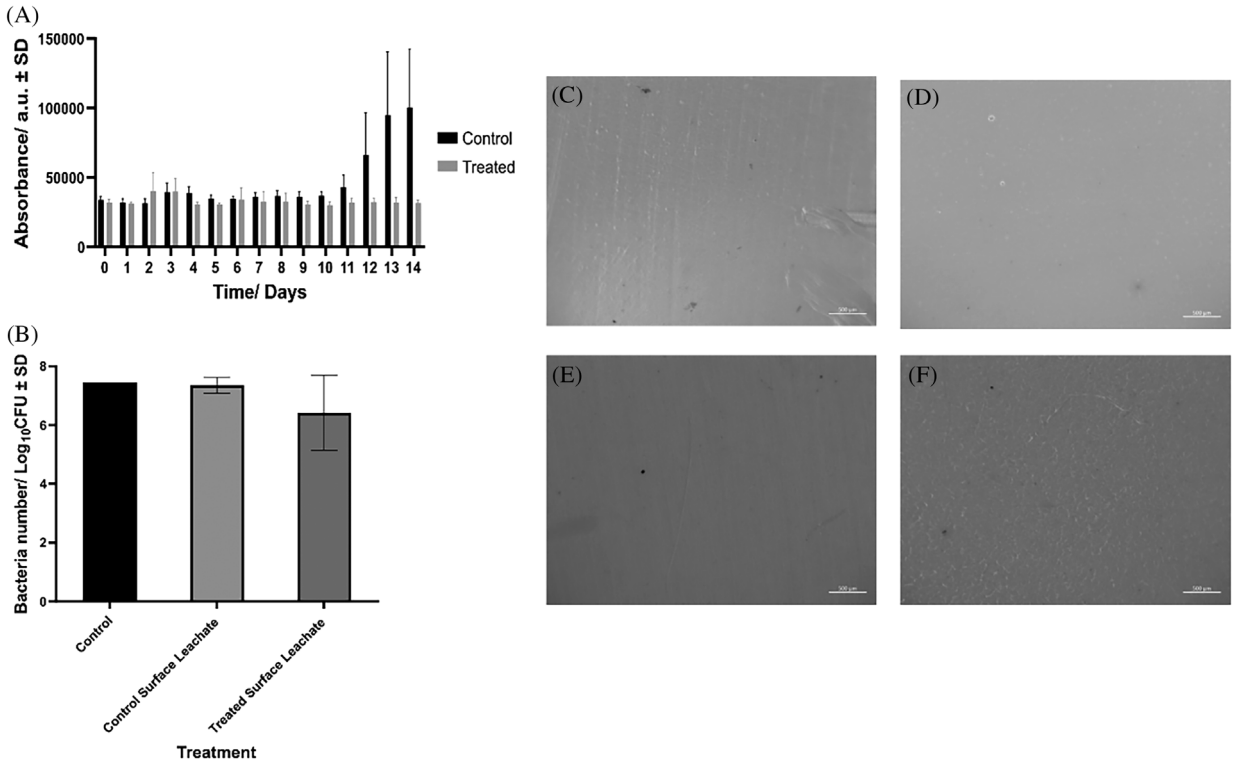

FIGURE 5 Durability of surfaces. A) Absorbance of leachate from treated and control surfaces to determine chlorhexidine leaching from surfaces. $N = 9$, error bars show standard deviation. B) Antimicrobial efficacy of the leachate from control and treated samples. $N = 9$, error bars show standard deviation. C–F) Light micrographs of the pre and post leaching surfaces. C) Control surface pre-leaching, D) control surface post-leaching, E) treated surface pre-leaching, F) treated surface post leaching. Images are representative of all samples scale bar is 500 μm.

ing level across all days. With the control samples, the absorbance remained level until day 12, when an increasing trend with high variability began to emerge. However, there was no significant difference between any time point and day 0.

To confirm this result, the surface leachate was tested against *E. coli*. While there was a slight decrease in the leachate from the treated surfaces, this was not significant, and no significant changes in bacterial growth were observed across all the samples. Finally, both control and treated surfaces were imaged pre- and post-leaching. Both control and treated surfaces showed some surface disruption after being in the leaching solution for 14 days (Figure 5C–F).

4 | DISCUSSION

Plasma nitriding of surfaces is an established technique that has previously been used to increase the hardness and wear resistance of surfaces and enhance cell attachment.[35,36] In this paper, we have reported utilizing this surface modification as the basis for attaching chlorhexidine to the surface to incorporate novel properties. Chlorhexidine, as a broad-spectrum biocide, is active against various organisms, including opportunistic pathogens responsible for disease. Therefore, covering the surface with a uniform chlorhexidine coating is key to developing strong antimicrobial properties. ToF-SIMS detection of the $C_7H_4N_2Cl^-$ ion is a key indicator of the presence of chlorhexidine in a system and demonstrates even coverage of our surfaces with the biocide.

We have previously demonstrated that it is possible to nitride metal surfaces and utilize the nitride layer as a functionalized surface to attach biocides.[28] Plasma nitriding of polymers is uncommon because it does not confer the same wear resistance properties seen in metals. The process normally requires extreme temperatures to modify steel surfaces. Therefore, we aimed to apply the nitriding process to thermally-sensitive polymers and attach biocides in a manner analogous to metals.

The presence of the biocidal coating does not affect the macrostructure of the material. However, it does alter the hydrophobicity of the surface. This is key for bacterial interactions with the surface, as hydrophobicity can reduce bacterial attachment.[37] Studies have shown that altering the surface to include more hydrophobic groups reduces bacterial survival. However, adding chlorhexidine

to the surfaces significantly reduced the water contact angle despite increasing the biocidal activity. This is thought to be due to the introduction of multiple cationic groups across the surface, increasing the hydrophilicity, and reducing bacterial attachment.[38]

Transmission of bacteria through fomites is a significant issue in healthcare, with up to 40% of nosocomial infections occurring from infected healthcare operatives' hands and via high-touch environmental surfaces. High-frequency touch surfaces require rapid antimicrobial action, and this is not limited to healthcare environments as fomite transmission of pathogenic species rapidly spreads in other environments.[39] This calls for technologies that can rapidly prevent the growth and survival of a range of pathogenic species. This is essential as studies have shown that as low as 15 CFU of *S. aureus* is required to cause infection.[40] The results we describe in this work demonstrate that chlorhexidine-coated surfaces show a rapid reduction in bacterial numbers for both Gram-negative (*E. coli*) and Gram-positive (*S. aureus*) organisms after 45 minutes. The antimicrobial effect was stronger against *C. albicans*, with no recoverable cells obtained after 15 minutes. This is significantly quicker than comparative technologies such as silver and copper, which reduce microbial numbers over hours or even days.[41–43] Studies have shown that, although SARS-CoV-2 is predominantly transmitted through respiratory and air transmission, the virus persists on surfaces, and fomite transmission is possible.[44,45] While chlorhexidine in solution has shown limited efficacy against the virus,[46] it has shown efficacy against SARS-CoV-2 in vivo.[47] Additionally, studies have shown that chlorhexidine attached to a surface can rapidly inactivate the virus.[29] We have shown that chlorhexidine immobilized on surfaces leads to a rapid reduction in viable virions and that this technology is applicable to polymer surfaces.

The development of chlorhexidine-resistant bacterial inoculants as a result of progressive bacterial isolate survival in sub-inhibitory concentrations of chlorhexidine was the result of permanent de novo genomic alterations mutated in response to antimicrobial stress and inherited by bacterial progeny following replication.[48,49] Previous experimental studies[50,51] further support the results obtained for developing chlorhexidine-resistant bacterial inoculants. Gradually increasing sub-inhibitory concentrations of chlorhexidine to *E. coli* and *S. aureus* progenitors induces selective pressure, upregulating the antimicrobial tolerance of repeat-specific isolates to a statistically significant degree.

The results of surface efficacy tests conducted further demonstrate that treated surfaces exhibit statistically significant bactericidal efficacy. The lack of survival of both naïve and resistant bacterial isolates after inoculation onto the antimicrobial surface was significant. It should be emphasized that this conclusion is limited to bacterial isolates exhibiting a chlorhexidine tolerance equal to or less than 32 μg mL^{-1}; however, recent studies investigating the in situ development of chlorhexidine resistance in bacterial isolates obtained from HCAI-patient wounds and patient-care fomites have provided evidence supporting the extent of healthcare-associated chlorhexidine resistance to be ≤8 μg mL^{-1}.[52]

While the majority of antimicrobial technologies used in infrastructure materials work by leaching antimicrobials from the surface,[53] the chlorhexidine used in the technology reported here is bonded to the surface, and leaching of the chlorhexidine was not observed. This lack of leaching from the surface could potentially enhance the duration of antimicrobial efficacy against bacteria, especially resistant strains, which often rely on efflux pumps to remove antimicrobials. However, further studies will be required to test this hypothesis. This suggests that the technology could potentially be used for wet environments. However, further studies would need to be carried out this as literature sources suggest alternative detection methods and changing washing conditions would be important to confirm this to its fullest extent.[54,55]

5 | CONCLUSION

Using a simple process, we have demonstrated a method for applying an established biocide to polymer surfaces. The coating of the surface is uniform across the surface. It shows excellent efficacy against both Gram-positive and Gram-negative bacteria, as well as against pathogenic fungi and enveloped viruses. We have developed two strains of chlorhexidine-resistant bacteria and shown that the technology demonstrates the same level of efficacy against chlorhexidine-resistant bacteria as naïve bacteria. We believe that the technology is widely applicable to prevent the spread of fomite infection.

ACKNOWLEDGEMENTS

This work was funded by the BBSRC via the National Biofilm Innovation Centre, the BBSRC funded Doctoral Training Centre, and the Royal Academy of Engineering Enterprise Fellowship. The authors gratefully acknowledge the assistance of Dr. Henri Huppert, Thermo Fisher Scientific, UK, for his help in developing automated quantification algorithms. In addition, they thank Dr. Graeme Forster, NitroPep, for providing nitrided surfaces used in this study. The Host and Pathogen Interactions group at the University of Birmingham provided *Candida albicans* SC5314. SARS-CoV-2-England 2 (Wuhan strain) virus

at 10^6 IU/mL (GSAID Accession ID EPI_ISL_407073) was a kind gift from Christine Bruce, Public Health England.

CONFLICT OF INTEREST

Dr. Felicity de Cogan was a founder of the company NitroPep Ltd. NitroPep Ltd. provided nitrided surfaces to allow this work to take place as detailed above.

DATA AVAILABILITY STATEMENT

Data is available upon reasonable request in line with journal policies.

REFERENCES

1. A. L. Andrady, M. A. Neal, *Philos. Trans. R Soc. B Biol. Sci.* **2009**, *364*, 1977.
2. E. J. North, R. U. Halden, *Rev. Environ. Health* **2013**, *28*, 1.
3. S. J. Dancer, *Clin. Microbiol. Rev.* **2014**, *27*, 665.
4. A. N. Neely, M. P. Maley, *J. Clin. Microbiol.* **2000**, *38*, 724.
5. A. N. Neely, *J. Burn Care Rehabil.* **2000**, *21*, 523.
6. V. Rebic, N. Masic, S. Teskeredzic, M. Aljicevic, A. Abduzaimovic, D. Rebic, *Med. Arch.* **2018**, *72*, 325.
7. A. N. Neely, M. M. Orloff, *J. Clin. Microbiol.* **2001**, *39*, 3360.
8. L. Aslanyan, D. Sanchez, S. Valdebenito, E. Eugenin, R. Ramos, L. Martinez, *J. Fungi.* **2017**, *3*, 10.
9. T. Benaducci, C. O. Sardi de, N. M. S. Lourencetti, L. Scorzoni, F. P. Gullo, S. A. Rossi, J. B. Derissi, M. C. de Azevedo Prata, A. M. Fusco-Almeida, M. J. S. Mendes-Giannini, *Front. Microbiol. [Internet]* **2016** [cited 2022 Sep 22], *7*. Available from: http://journal.frontiersin.org/Article/10.3389/fmicb.2016.00290/abstract
10. D. E. Corpet, *Med. Hypotheses* **2021**, *146*, 110429.
11. Y. Pan, D. Zhang, P. Yang, L. L. M. Poon, Q. Wang, *Lancet Infect. Dis.* **2020**, *20*, 411.
12. G. M. Knight, T. M. Pham, J. Stimson, S. Funk, Y. Jafari, D. Pople, S. Evans, M. Yin, C. S. Brown, A. Bhattacharya, R. Hope, M. G. Semple, ISARIC4C Investigators, CMMID COVID-19 Working Group, J. M. Read, B. S. Cooper, J. V. Robotham, *BMC Infect. Dis.* **2022**, *22*, 556.
13. J. F. Guest, T. Keating, D. Gould, N. Wigglesworth, *BMJ Open* **2020**, *10*, e033367.
14. J. Carter, *Health Stat. Q.* **2009**, *43*, 38.
15. B. S. Cooper, G. F. Medley, S. P. Stone, C. C. Kibbler, B. D. Cookson, J. A. Roberts, G. Duckworth, R. Lai, S. Ebrahim, *Proc. Natl. Acad. Sci. U S A* **2004**, *101*, 10223.
16. J. D. Edgeworth, R. Batra, J. Wulff, D. Harrison, *Clin. Infect. Dis.* **2020**, *70*, 2530.
17. V. Russotto, A. Cortegiani, S. M. Raineri, A. Giarratano, *J. Intensive Care* **2015**, *3*, 54.
18. I. Francolini, I. Silvestro, V. Di Lisio, A. Martinelli, A. Piozzi, *Int. J. Mol. Sci.* **2019**, *20*, 1001.
19. X.-T. Wang, X. Deng, T.-D. Zhang, J. Zhang, L.-L. Chen, Y.-F. Wang, X. Cao, Y.-Z. Zhang, X. Zheng, *ACS Macro Lett.* **2022**, *11*, 805.
20. D. S. Jones, C. P. Garvin, D. Dowling, K. Donnelly, S. P. Gorman, *J. Biomed. Mater. Res. B Appl. Biomater.* **2006**, *78B*, 230.
21. A.W. Zia, I. Anestopoulos, M. I. Panayiotidis, M. Birkett, *Ceram. Int.* **2023**, *49*, 17203.
22. K. Yonezawa, M. Kawaguchi, A. Kaneuji, T. Ichiseki, Y. Iinuma, K. Kawamura, K. Shintani, S. Oda, M. Taki, N. Kawahara, *Antibiotics* **2020**, *9*, 495.
23. T. Juknius, M. Ružauskas, T. Tamulevičius, R. Šiugždinienė, I. Juknienė, A. Vasiliauskas, A. Jurkevičiūtė, S. Tamulevičius, *Materials* **2016**, *9*, 371.
24. H.-X. Wu, L. Tan, Z.-W. Tang, M.-Y. Yang, J.-Y. Xiao, C.-J. Liu, R.-X. Zhuo, *ACS Appl. Mater. Interfaces* **2015**, *7*, 7008.
25. S. Skovgaard, L. N. Nielsen, M. H. Larsen, R. L. Skov, H. Ingmer, H. Westh, Webber MA editor, *PLoS One* **2013**, *8*, e62197.
26. D. E. Carey, P. J. McNamara, *Front. Microbiol. [Internet]* **2015**, *780*. Available from: http://journal.frontiersin.org/article/10.3389/fmicb.2014.00780/abstract
27. L. Riordan, E. F. Smith, S. Mills, J. Hudson, S. Stapley, N. Nikoi, S. Edmondson, J. Blair, A. F. A. Peacock, D. Scurr, G. Forster, F. de Cogan, *Mater Sci. Eng. C* **2019**, *102*, 299.
28. J. A. Bryant, L. Riordan, R. Watson, N. D. Nikoi, W. Trzaska, L. Slope, C. Tibbatts, M. R. Alexander, D. J. Scurr, R. C. May, F. de Cogan, *Glob. Chall.* **2022**, *6*, 2100138.
29. R. Watson, M. Oldfield, J. A. Bryant, L. Riordan, H. J. Hill, J. A. Watts, M. R. Alexander, M. J. Cox, Z. Stamataki, D. J. Scurr, F. de Cogan, *Sci. Rep.* **2022**, *12*, 2803.
30. J. Naderi, C. Giles, S. Saboohi, H. J. Griesser, B. R. Coad, *Biointerphases* **2018**, *13*, 06E409.
31. J. M. Andrews, *J. Antimicrob. Chemother.* **2001**, *48*, 5.
32. A. M. Holmes, D. J. Scurr, J. R. Heylings, K.-W. Wan, G. P. Moss, *Eur. J. Pharm. Sci.* **2017**, *104*, 90.
33. A. M. Judd, D. J. Scurr, J. R. Heylings, K.-W. Wan, G. P. Moss, *Pharm. Res.* **2013**, *30*, 1896.
34. T. Attin, T. Abouassi, K. Becker, A. Wiegand, M. Roos, R. Attin, *Clin. Oral Investig.* **2008**, *12*, 189.
35. H. Hänninen, J. Romu, R. Ilola, J. Tervo, A. Laitinen, *J. Mater. Process. Technol.* **2001**, *117*, 424.
36. R. del Castillo, K. Chochlidakis, P. Galindo-Moreno, C. Ercoli, *J. Prosthodont.* **2022**, *31*, 571.
37. K. Kuroda, G. A. Caputo, W. F. DeGrado, *Chem. - Eur. J.* **2009**, *15*, 1123.
38. U. Mahanta, M. Khandelwal, A. S. Deshpande, *J. Mater. Sci.* **2021**, *56*, 17915.
39. H. Lei, Y. Li, S. Xiao, X. Yang, C. Lin, S. L. Norris, D. Wei, Z. Hu, S. Ji, *Sci. Rep.* **2017**, *7*, 14826.
40. W. D. Foster, M. S. R. Hutt, *Lancet* **1960**, *276*, 1373.
41. C. Bankier, R. K. Matharu, Y. K. Cheong, G. G. Ren, E. Cloutman-Green, L. Ciric, *Sci. Rep.* **2019**, *9*, 16074.
42. E. T. Enan, A. A. Ashour, S. Basha, N. H. Felemban, S. M. F. Gad El-Rab, *Nanotechnology* **2021**, *32*, 215101.
43. C. Gangwar, B. Yaseen, R. Nayak, S. Praveen, N. Kumar Singh, J. Sarkar, M. Banerjee, *Inorg. Chem. Commun.* **2022**, *141*, 109532.
44. H. A. Aboubakr, T. A. Sharafeldin, S. M. Goyal, *Transbound Emerg. Dis.* **2021**, *68*, 296.
45. M. Marquès, J. L. Domingo, *Environ. Res.* **2021**, *193*, 110559.
46. G. Kampf, D. Todt, S. Pfaender, E. Steinmann, *J. Hosp. Infect.* **2020**, *104*, 246.
47. Y. H. Huang, J. T. Huang, *J. Med. Virol.* **2021**, *93*, 4370.
48. M. Frieri, K. Kumar, A. Boutin, *J. Infect. Public Health* **2017**, *10*, 369.
49. A. B. Janssen, D. van Hout, M. J. M. Bonten, R. J. L. Willems, W. van Schaik, *J. Antimicrob. Chemother.* **2020**, *75*, 3135.

50. P. Parvekar, J. Palaskar, S. Metgud, R. Maria, S. Dutta, *Biomater. Investig. Dent.* **2020**, *7*, 105.
51. G. Royer, L. Poirel, B. La Combe, O. Clermont, F. Chau, M. Mercier-Darty, E. Denamur, P. Nordmann, J.-D. Ricard, J.-W. Decousser, *J. Antimicrob. Chemother.* **2021**, *76*, 2736.
52. T. M. Bes, L. Perdigão-Neto, R. R. Martins, I. Heijden, T. P. A, G. Camilo, D. S. Nagano, D. Mongelos, A. P. Marchi, M. Tomaz, L. M. de Oliveira, F. Rossi, A. S. Levin, S. F. Costa, *Rev. Inst. Med. Trop. São Paulo* **2021**, *63*, e27.
53. Z.-T. Hu, Y. Chen, Y.-F. Fei, S.-L. Loo, G. Chen, M. Hu, Y. Song, J. Zhao, Y. Zhang, J. Wang, *Sci. Total Environ.* **2022**, *837*, 155720.
54. C. H. Ho, E. K. Odermatt, I. Berndt, J. C. Tiller, *J. Biomater. Sci. Polym. Ed.* **2013**, *24*, 1589. https://doi.org/10.1080/09205063.2013.782803
55. A. Strassburg, J. Petranowitsch, F. Paetzold, C. Krumm, E. Peter, M. Meuris, M. Köller, J. C. Tiller, *ACS Appl. Mat. Inter.* **2017**, *9*, 36573. https://doi.org/10.1021/acsami.7b10049
56. Y. Imai, K. J. Meyer, A. Iinishi, Q. Favre-Godal, R. Green, S. Manuse, M. Caboni, M. Mori, S. Niles, M. Ghiglieri, C. Honrao, X. Ma, J. J. Guo, A. Makriyannis, L. Linares-Otoya, N. Böhringer, Z. G. Wuisan, H. Kaur, R. Wu, A. Mateus, A. Typas, M. M. Savitski, J. L. Espinoza, A. O'Rourke, K. E. Nelson, S. Hiller, N. Noinaj, T. F. Schäberle, A. D'Onofrio, K. Lewis, *Nature* **2019**, *576*, 4594.

How to cite this article: R. Watson, M. Maxwell, S. Dunn, A. Brooks, L. Jiang, H. J. Hill, G. Williams, A. Kotowska, N. D. Nikoi, Z. Stamataki, M. Banzhaf, D. Scurr, J. A. Bryant, F. de Cogan, *Nano Select*. **2023**, 1.
https://doi.org/10.1002/nano.202300005